

Dynamics of the Higher Lying Excited States of Cyanine Dyes. An Ultrafast Fluorescence Study

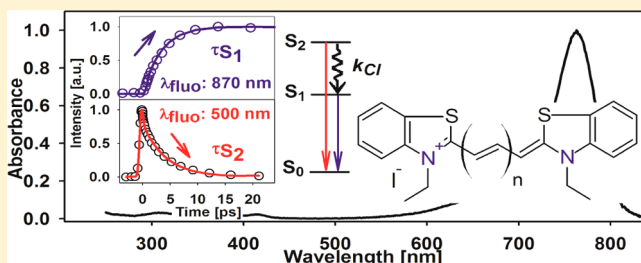
Cesar A. Guarin, Juan. P. Villabona-Monsalve, Rafael López-Arteaga, and Jorge Peon*

Instituto de Química, Universidad Nacional Autónoma de México, Circuito Exterior, Ciudad Universitaria, México, 04510, D.F., México

S Supporting Information

ABSTRACT: The electronic relaxation dynamics of the second singlet excited states of several cyanine dyes was studied through the femtosecond fluorescence up-conversion technique. Our interest in these molecules comes from the potential applications of systems with upper excited singlet states with a long lifetime, which can include electron and energy transfer from the higher lying singlets after one- or two-photon absorption. We studied three series of cyanines with 4-quinolyl, 2-quinolyl, or benzothiazolyl type end groups, each with varying sp^2 carbon conjugation lengths in the methinic bridge.

The dynamics after electronic excitation to singlet states above the fluorescent state vary significantly as a function of cyanine structure and conjugation length. In particular, for the 4-quinolyl series the cyanine with an intermediate conjugation length (three methinic carbons) has the slowest S_2 decays with lifetimes of 5.4 ps in ethanol and 6.6 ps in ethylene glycol. On the other hand, we observed that the 2-quinolyl family has S_2 decay times in the subpicosecond range independent of the conjugation length between the end groups. The slowest internal conversion was observed for the benzothiazolyl type cyanine with five methinic carbons, with an S_2 lifetime of 17.3 ps in ethanol. For the planar cyanines of this study we observed for the first time a clear systematic trend in the S_2 decay times which closely follow the energy gap law. It was also demonstrated that a slow S_2 decay is as well observed upon excitation through degenerate two-photon absorption with near-IR pulses. The present study isolates the most important variables for the design of cyanines with long S_2 lifetimes.



INTRODUCTION

Cyanines are polymethinic dyes with a positive charge delocalized through a chain of sp^2 carbons with amino end groups. Because of their extended conjugation, these systems have found multiple applications including optical storage and processing,¹ imaging of biological samples,^{2–4} light-energy conversion,^{5,6} nonlinear optics,⁷ optical limiting,⁸ sensitization,⁹ etc. The electronic structure of cyanines is determined by an odd number of conjugated p_z orbitals and an even number of π electrons associated with them.^{10,11} The resulting nodal structure of the π and π^* orbitals in these systems makes the first singlet excited state be significantly stabilized in comparison with the S_2 state. Spectroscopically, the electronic structure of these dyes produces an intense S_0 – S_1 transition in the visible or near-IR region and much less intense S_0 – S_n ($n \geq 2$) transitions in the near-UV region.¹¹

Since the S_2 – S_1 energy gap in some cyanines can be as large as 1 eV, the coupling between these states is significantly reduced in comparison with typical chromophores.¹² Besides the energy relations, it has been pointed out that due to their size, a kind of structural inertia in these molecules redounds in slow structural relaxation which may imply that the energy surface of the upper states is explored slowly after excitation.¹³ The slow S_2 – S_1 internal conversion observed in certain cyanine dyes^{14–16} can be explained by the above-mentioned features;

however, to this date no direct and accurate measurement of the higher lying singlet lifetimes or a systematic study about the factors that govern the upper state dynamics in different cyanines has been made.

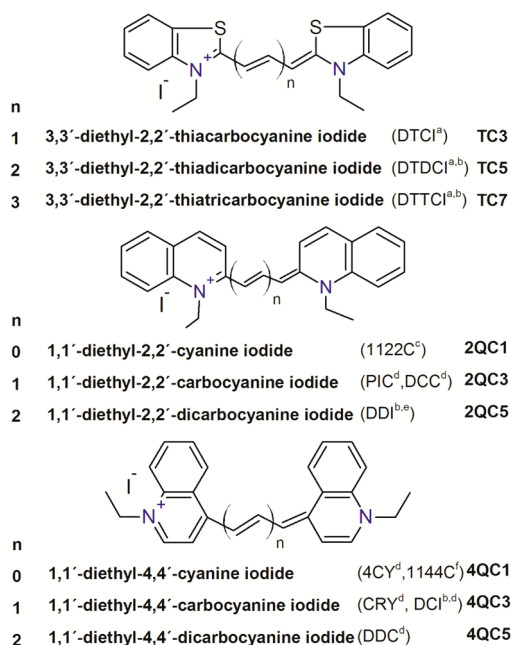
In this contribution we report on direct measurements of the lifetimes of the second excited singlet states of three cyanine families each with varying conjugation lengths. We studied these series in order to determine the structural features that contribute to a slow internal conversion from S_2 . We focused on the photophysics of cyanines with the following end groups: 4-quinolyl, 2-quinolyl, and benzothiazolyl. The structures of these cyanines are summarized in Scheme 1 together with the abbreviations used herein and in previous studies.

Molecules with a long-lived upper excited state could have significant applications since the energy available through the population of the upper singlets can be significantly larger than that of the S_1 state (around 3 eV for the S_2 state in certain cyanines against 1.5–2 eV for the S_1 state). This has been proven to redound in interesting electron transfer schemes in different molecular systems.^{13,17–20} Also, the long S_2 lifetimes

Received: January 9, 2013

Revised: May 14, 2013

Scheme 1. Molecular Structure and Abbreviations for the Cyanines of This Study (Abbreviations Used in Previous Publications Are Indicated in Parentheses)



^aReference 45. ^bReference 16. ^cReference 43. ^dReference 55. ^eReference 41. ^fReference 37.

in certain cyanines are related to applications like optical limiting.^{16,21,22}

Cyanine dyes have an additional aspect that makes them interesting in regards to their upper states: Because of the symmetry relations between their ground, first excited, and upper excited states, it has been shown extensively that these compounds have considerably large two-photon absorption cross sections for near-IR wavelengths (for example, for C_{2v} symmetry, $S_0: A_1, S_1: B_1, S_2: A_1$ for a near-resonant two-photon process with an intermediate state).^{23–26} These symmetry relations go in addition to an intense one-photon allowed first transition with a sharp onset in the near-IR which augments their nonlinear absorption for photons near the S_1 edge.^{24,26–28} Such ease to form the upper electronic states through two-photon absorption, together with the relatively long lifetime of these states, opens the possibility of interesting applications in which the cyanines may transfer energy from their upper states to other chromophores after two-photon excitation of the cyanine. Such a concept of a two-photon photosensitizer or antenna requires as a first step the kind of characterization of the present studies to understand and predict which type of cyanines may have a long-lived S_2 state.

The experiments presented herein determine the dynamics of the upper states by exciting the compounds in the UV region (266 or 400 nm), which correspond to direct excitations to the second singlet S_2 or higher lying singlets S_n ($n > 2$). We followed the upper state dynamics by time-resolving the transient spontaneous emission from the second singlet excited states using the femtosecond fluorescence up-conversion technique. Additionally, we monitored the population growth of the first singlet excited state (forming from internal conversion) by resolving the emission from the S_1 fluorescent state. These experiments were able to observe for the first time in a direct way the one to one kinetics of the S_2 – S_1 internal

conversion. Our results also show for the first time clear differences about the upper state relaxation times of the different cyanine series and the dependence on their conjugated skeleton size. As we show, the S_2 lifetimes can vary by more than 2 orders of magnitude depending on the system size and the kind of end groups. In order to determine the feasibility of producing a long-lived upper state through two-photon excitation, we also include experiments that form the upper singlets by degenerate two photon excitation in the near-IR (800 nm), demonstrating that the long-lived S_2 states may also be formed by nonlinear excitation.

EXPERIMENTAL SECTION

Materials. The cyanines in Scheme 1 were purchased from Aldrich and were used after extensive recrystallization from methanol and the solvent mixture dichloromethane–ether, until large high-purity crystal samples were obtained. After the purification stage, the samples were kept in dark conditions before the laser studies. HPLC quality solvents from Aldrich were used.

Synthesis of 2-(2-(2-Chloro-3-[2-(3-ethyl-3H-benzothiazol-2-ylidene)ethylidene]cyclohex-1-enyl)(vinyl)-3-ethylbenzothiazol-3-ium iodide (Cl-TC7). This dye (Cl-TC7) was synthesized from a solution of 1.6 g of 3-ethyl-2-methylbenzothiazolium iodide, 0.75 g of *N*-[(3-(anilino-methylene)-2-chloro-1-cyclohexen-1-yl)methylene]aniline monohydrochloride, and 0.47 g of sodium acetate in 100 mL of absolute ethanol. The mixture was heated under reflux for 20 min. After cooling overnight at $-5\text{ }^{\circ}\text{C}$, the resulting crystals were washed with water, cold ethanol, and diethyl ether.²⁹ Green crystals were obtained after recrystallization from methanol. Yield 70%; mp $269\text{ }^{\circ}\text{C}$; λ_{max} (ethanol) = 798.5 nm. The NMR spectra was compared with the one reported by Li et al.³⁰

Optical Spectroscopy. The steady state absorption spectra were acquired in a Cary-50 (Varian) spectrophotometer, and for the emission spectra, a Cary Eclipse (Varian) fluorimeter was used. The emission and excitation spectra were corrected for the instrumental response. All experiments were performed at room temperature ($20 \pm 1\text{ }^{\circ}\text{C}$) under aerated conditions. For the emission measurements from the upper states, the absorption at the excitation wavelength was kept below 0.05, except for the 2QC series, 4QC1, and TC3 for which higher concentrations were necessary in order to observe the emission from the higher lying states. For these cyanines, the absorbance at the excitation wavelength was of 0.15.

The femtosecond fluorescence up-conversion setup has been described previously.^{31–34} It is based on a regeneratively amplified, 1 kHz Ti:sapphire laser centered at 800 nm, producing a 0.7 W pulse train of 150 fs in duration. The second or third harmonic was used for excitation and was obtained by sum frequency mixing in 0.5 mm β -BBO crystals. The samples were studied in 1 mm flow cells, and the fluorescence was collected with a pair of parabolic mirrors and refocused to the up-conversion β -BBO crystal where it was crossed with $\sim 1\text{ mW}$ of the 800 nm fundamental beam split previously. The sum frequency signal was collected with a CaF_2 lens and focused into a double 10 cm monochromator (Oriel) and detected with a photomultiplier tube. The excitation beam was modulated at 1/3 of the laser repetition rate with a phase-locked chopper, so that the up-conversion signal could be detected with a lock-in amplifier (Stanford Research Systems). The polarization of the excitation pulses was adjusted with wave

plates for magic angle conditions with respect to the up-conversion crystal (type I sum frequency process, detecting the vertical component of the fluorescence intensity). The instrument response functions (IRF) for the up-conversion experiments were determined to be Gaussian with a full width at half-maximum of 450 fs for 400 nm excitation and 500 fs for 266 nm excitation.^{31–33} From the inspection of exponential functions convoluted with these instrumental response functions and considering the signal-to-noise ratio of our experiments, the shortest lifetimes that can be measured with this setup have time constants of $\sim 40\%$ of the respective IRF. Some of the emission decay times in this contribution are reported as being below this instrumental limit. For all up-conversion experiments, solvent-only traces were taken back-to-back and with identical alignment to the solution measurements to ensure the absence of signals near $t = 0$ due to scattering from the solvent.

RESULTS AND DISCUSSION

Steady State Spectroscopy. Figures 1–3 show the steady state absorption and emission spectra of the molecules of

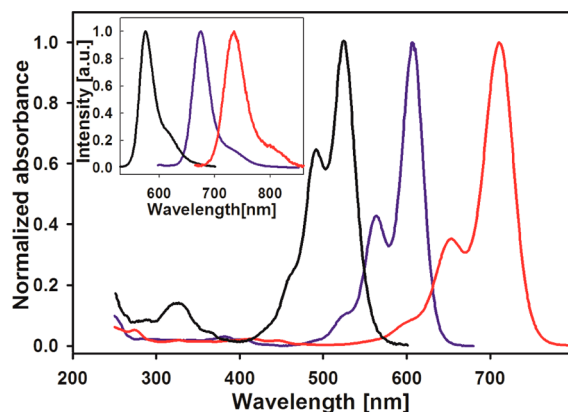


Figure 1. Absorption (main graph) and emission (inset) spectra of cyanines 2QC1 (black), 2QC3 (blue), and 2QC5 (red) in ethanol solution.

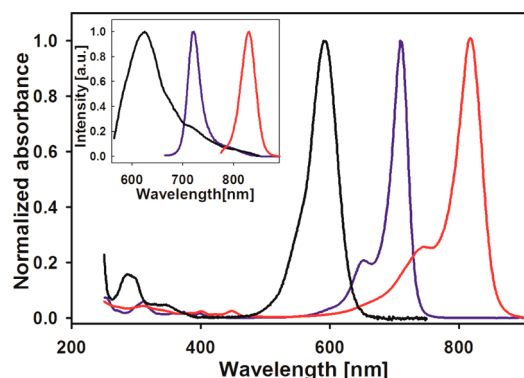


Figure 2. Absorption (main graph) and emission (inset) spectra of cyanines 4QC1 (black), 4QC3 (blue), and 4QC5 (red) ethanol solution.

Scheme 1 in ethanol solution. For the three cyanine series, it can be seen that the first and higher transitions undergo systematic shifts when the conjugation length is changed. However, the S_0 – S_1 absorptions undergo somewhat different shifts as the polymethinic length is increased in comparison

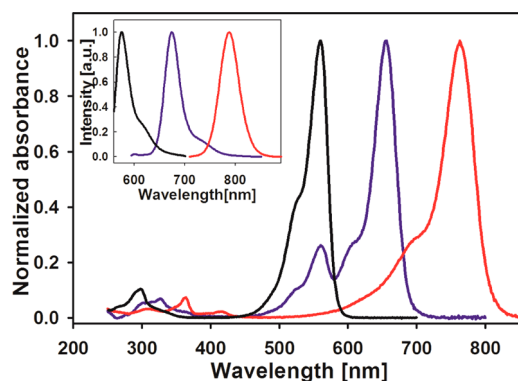


Figure 3. Absorption (main graph) and emission (inset) spectra of cyanines TC3 (black), TC5 (blue), and TC7 (red) in ethanol solution.

with the transitions at higher energies. This redounds changes in the S_2 – S_1 gap as the polymethinic chain increases. The quantification and dynamical effects of this observation are presented in a latter paragraph.

Figure 4 shows emission spectra in the visible range, in the region between the first and second absorption transitions for

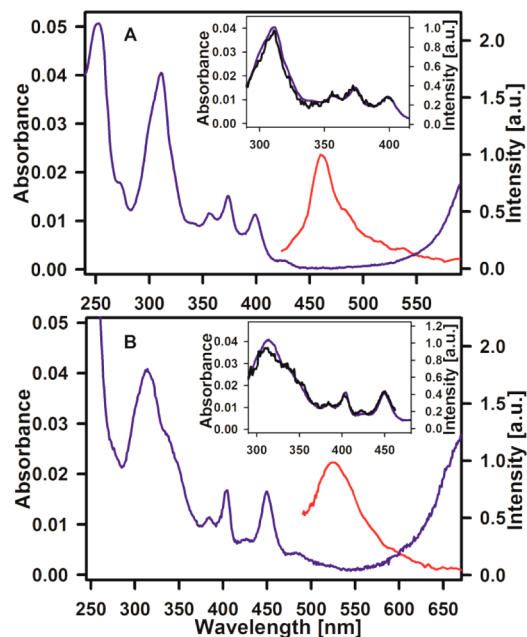


Figure 4. Corrected emission spectra from the S_2 state (red), absorption (blue), and corrected excitation spectra (black, insets) for 4QC3 (A, $\lambda_{\text{exc}} = 400$ nm, $\lambda_{\text{det}} = 460$ nm) and 4QC5 (B, $\lambda_{\text{exc}} = 450$ nm, $\lambda_{\text{det}} = 540$ nm).

4QC3 and 4QC5. As can be seen, a clear emission is detected with peaks at 460 nm for 4QC3 and 523 nm for 4QC5. The respective emission spectra for 4QC1, TC3, and the 2QC series are included in the Supporting Information. From the position of the emission bands in Figure 4 and the excitation spectra (see below), such fluorescence signals can be readily assigned to the radiative decay of the S_2 states of the respective cyanines.^{14,16} Similarly, for the benzothiazolyl type cyanines (TC series), the fluorescence spectra in the 400–600 nm region show clear emission peaks with maxima at 429 nm for TC5 and 494 nm for TC7 as shown in Figure 5. As in the case of the 2QC series, for the shortest cyanine TC3, weak S_2

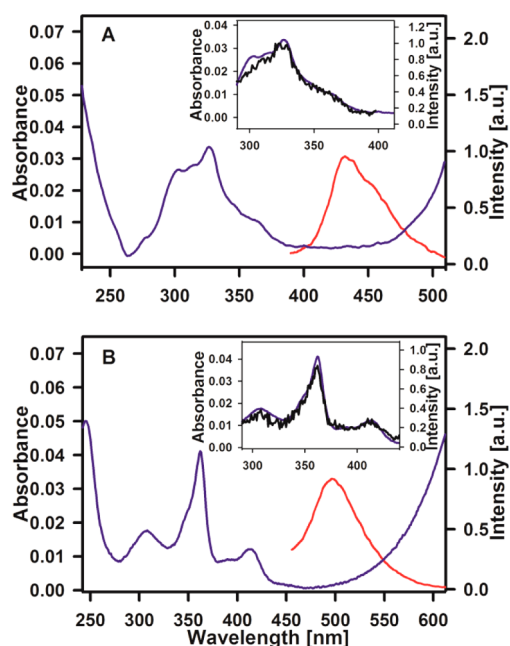


Figure 5. Corrected emission spectra from the S_2 state (red), absorption (blue), and corrected excitation spectra (black, insets) for TC5 (A, $\lambda_{\text{exc}} = 330$ nm, $\lambda_{\text{det}} = 450$ nm) and TC7 (B, $\lambda_{\text{exc}} = 365$ nm, $\lambda_{\text{det}} = 490$ nm).

emission is observed only with somewhat more concentrated solutions with an absorbance of 0.15 at the excitation wavelength (see Supporting Information). The quantum yields for the S_2 emissions of all cyanines were determined to be $\Phi_{\text{fluor}} < 10^{-3}$ from comparisons with the emissions of coumarin 153 and coumarin 343.

The excitation spectra with detection near the S_2 emission maxima for 4QC3, 4QC5, TC5, and TC7 are shown in the respective insets of Figures 4 and 5. As can be seen, the absorption features for the UV regions of the four molecules are reproduced, indicating that the emission does not come from an impurity. From the normalization of the excitation spectra to the absorption spectra at the respective longest wavelength vibroelectronic peaks (near the blue edge of the emissions, see insets), it is clear that the quantum yield for S_2 emission is nearly constant as the excitation wavelength was scanned through the band systems in the spectral regions depicted in the insets. This indicates that, considering that the multiple vibroelectronic absorption peaks on the blue side of the S_2 emission correspond to a series of different electronic states S_n ($n \geq 2$), the quantum yield for the formation of the transient emissive S_2 state is above $\sim 90\%$, implying a regular highly efficient S_n – S_2 internal conversion. This is further studied through femtosecond experiments with different excitation wavelengths shown below.

Time-Resolved Fluorescence. Femtosecond fluorescence up-conversion traces for the nine cyanines of Scheme 1 are included in Figures 6–8, and the results of their analysis are summarized in Table 1. The main graphs in these figures correspond to the time-resolution of the spontaneous emission from the S_2 states. Figure 6 shows the data for the 2QC series. For the 2QC3 and 2QC5 cyanines, an excitation wavelength of 400 nm was used, while 266 nm excitation was necessary to excite the upper singlets in 2QC1. As can be seen, using the up-conversion technique, ultrafast decaying transients in the S_2 emission region were well resolved despite the weak emissions

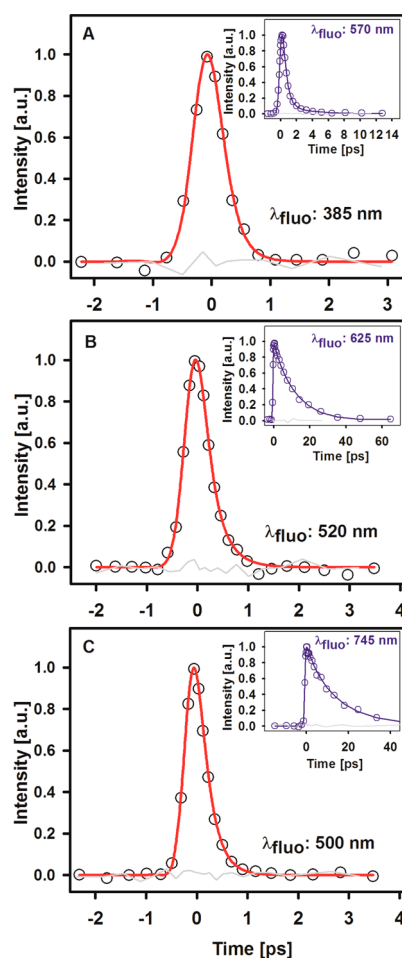


Figure 6. Femtosecond fluorescence up-conversion results with detection of the S_2 emission for 2QC1 (A, $\lambda_{\text{exc}} = 266$ nm), 2QC3 (B, $\lambda_{\text{exc}} = 400$ nm), and 2QC5 (C, $\lambda_{\text{exc}} = 400$ nm). Insets: time-resolved fluorescence from the S_1 state (blue). The detection wavelengths (λ_{fluor}) are indicated. The gray lines are the solvent-only scans.

in the steady state spectra. For this series, independent of the polymethinic chain length, the full decay of this state takes place within 1 ps, and the traces were described as a single-exponential decay with a time constant of $\tau < 0.2$ ps convoluted with our IRF ($\tau < 0.3$ ps for 2QC3). The insets of Figure 6 show the time-resolved emission from the “fluorescent” first singlet excited states of the 2QC cyanines. Consistent with the ultrafast S_2 decays, the S_1 emissions show an instrument limited rise ($\tau_{\text{rise}} < 0.3$ ps), followed by a single- or double-exponential decay. The S_1 decays in these and other cyanines have been extensively studied by several groups.^{35–45} The relatively short fluorescent state lifetimes in these systems is due to rapid fluctuations in the polymethinic chain leading to efficient isomerizations and/or internal conversion to the electronic ground state with the intermediacy of S_1 – S_0 conical intersections.^{35,36,38,42,43,46} Since the focus of this study are the S_2 dynamics, the S_1 time-resolved emission traces were acquired to verify the consistency of the kinetics of the population of the S_1 fluorescent state as the S_2 emission is depleted. In all cases, the S_1 lifetimes are consistent with the respective previous studies,^{35,36,38,42,43,46} while the S_2 decays are reported herein for the first time with femtosecond resolution.

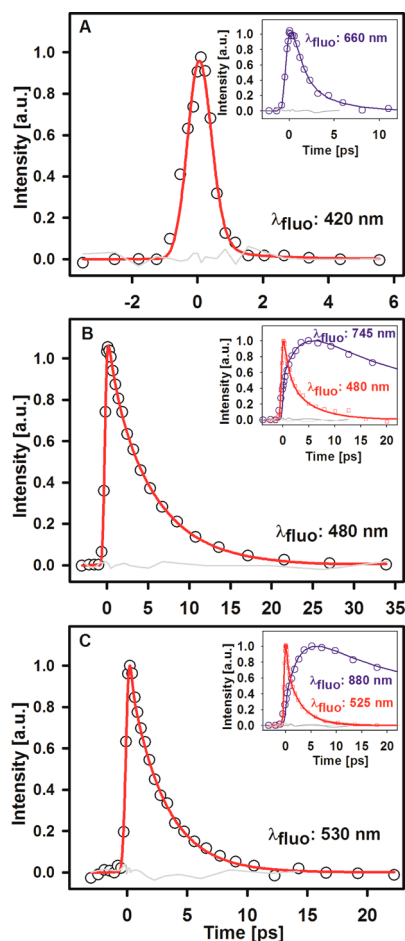


Figure 7. Femtosecond fluorescence up-conversion results with detection of the S_2 emission for 4QC1 (A, $\lambda_{\text{exc}} = 266$ nm), 4QC3 (B, $\lambda_{\text{exc}} = 400$ nm), and 4QC5 (C, $\lambda_{\text{exc}} = 400$ nm). Insets: time-resolved fluorescence from the S_1 state (blue) and from the S_2 state for 4QC3 (B) and 4QC5 (C) with 266 nm excitation (red). The detection wavelengths (λ_{fluo}) are indicated. The gray lines are the solvent-only scans.

The up-conversion results for the 4QC series are included in Figure 7. As can be seen, for this series there are important differences in comparison with the 2QC series, and there are also important changes in the dynamics as the polymethinic chain length is increased: the S_2 emission trace of the shortest cyanine, 4QC1, is similar to the respective results of the 2QC series. That is, there is an ultrafast decay of the emission signal in the visible region with an S_2 lifetime of $\tau < 0.4$ ps (detected at 420 nm, between the first and second absorption bands). Correspondingly, we observed an instrument limited rise of the S_1 fluorescence (660 nm), followed by its decay with a time constant of $\tau = 1.8$ ps.

For the 4QC3 cyanine, the S_2 fluorescence signal shows a much slower decay (see Figure 7B). This signal was followed at 480 nm and shows a biexponential decay with time constants of $\tau_1 = 1.0$ ps and $\tau_2 = 5.4$ ps. Such slow internal conversion and the steady state detection of the S_2 emission are clear exceptions to Kasha's rule.¹² The slow (picoseconds) decay of the S_2 state was also observed when the system was excited to an upper state S_n with 266 nm light instead of 400 nm light. This is shown in the red trace in the inset of Figure 7B. In this case, we observed a double-exponential decay with time constants of $\tau_1 = 0.9$ and $\tau_2 = 5.3$ ps. The similar time scales

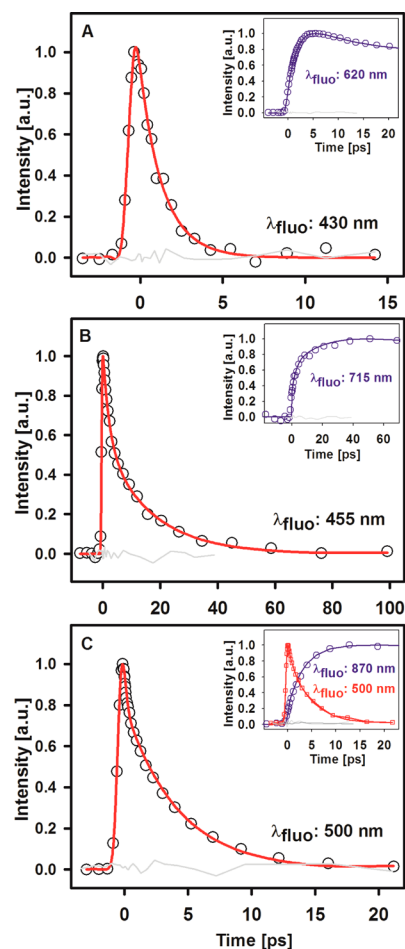


Figure 8. Femtosecond fluorescence up-conversion results with detection of the S_2 emission for TC3 (A, $\lambda_{\text{exc}} = 266$ nm), TC5 (B, $\lambda_{\text{exc}} = 266$ nm), and TC7 (C, $\lambda_{\text{exc}} = 400$ nm). Insets: time-resolved fluorescence from the S_1 state (blue) and from the S_2 state for TC7 (C) with 266 nm excitation (red). The detection wavelengths (λ_{fluo}) are indicated. The gray lines are the solvent-only scans.

to the 400 nm excitation show that even when different upper states are formed, the molecules nearly instantaneously form the second excited state where the population is retained for several picoseconds, giving rise to spontaneous emission signals from this state before it undergoes further internal conversion. It should be noted that the amplitude of τ_1 changes from 0.2 to 0.46 when changing the excitation wavelength from 400 to 266 nm. We consider that this is an indication that the first time constant is related to the early evolution of the system in the S_2 potential energy surface and that when the excitation energy is increased by 1.56 eV, this results in the formation of a population of molecules formed from internal conversion from the higher lying states (S_n , $n > 2$). Apparently, this results in a larger fraction of the systems evolving through a faster channel most likely related to the relaxation within the S_2 state (~ 1 ps). Overall, the biexponential nature of the emission decays in this zone is probably due to spectral modulations associated with the electronic and vibrational relaxation, and possibly, also from the fact that a fraction of the population may relax faster into the S_1 state—possibly a sign of structural inhomogeneity in the cyanine population. In any case, these experiments show that for 4QC3 there is a transient S_2 population following the

Table 1. Parameters for the Decay of the S_2 and S_1 States for the Cyanines of Scheme 1 in Ethanol Solutions

cyanine	state detected	λ_{fluor} [nm]	τ_1 [ps]	a_1	τ_2 [ps]	a_2	τ_3 [ps]	a_3
2QC1	S_2^a	385	<0.2	1				
2QC1	S_1^a	570	0.6 ± 0.02	0.96	5.1 ± 0.3	0.04		
2QC3	S_2^b	520	<0.3	1				
2QC3	S_1^a	625			11.9 ± 0.2	1		
2QC5	S_2^b	500	<0.2	1				
2QC5	S_1^a	745			14.3 ± 0.6	1		
4QC1	S_2^a	420	<0.4	1				
4QC1	S_1^a	660	<0.4	−0.42	1.8 ± 0.1	0.58		
4QC3	S_2^b	480	1.0 ± 0.05	0.20	5.4 ± 0.3	0.80		
4QC3	S_1^a	480	0.9 ± 0.3	0.46	5.3 ± 0.5	0.54		
4QC3	S_1^a	745	2.8 ± 0.2	−0.50	7.5 ± 0.9	0.26	57 ± 1	0.24
4QC5	S_2^b	530	0.5 ± 0.04	0.84	2.9 ± 0.1	0.16		
4QC5	S_2^a	525	<0.4	0.53	3.1 ± 0.1	0.47		
4QC5	S_1^a	880	3.0 ± 0.3	−0.50	10.0 ± 1.0	0.29	106 ± 8	0.21
TC3	S_2^a	430			1.5 ± 0.07	1		
TC3	S_1^a	620			2.2 ± 0.04	−0.49	155 ± 3	0.51
TC5	S_2^a	455	1.9 ± 0.06	0.49	17.3 ± 0.1	0.51		
TC5	S_1^a	715	2.0 ± 0.4	−0.26	17.2 ± 3.0	−0.24	562 ± 15	0.50
TC7	S_2^b	500	<0.3	0.53	4.3 ± 0.1	0.47		
TC7	S_2^a	500	0.8 ± 0.1	0.22	4.6 ± 0.2	0.78		
TC7	S_1^a	870	<0.2	−0.15	3.4 ± 0.2	−0.38	845 ± 18	0.47

^aExcitation wavelength (λ_{exc}): 266 nm. ^b λ_{exc} = 400 nm.

formation of the upper states with a lifetime of several picoseconds.

The time-resolved S_1 emission of 4QC3 at 745 nm is also included in the inset of Figure 7B (blue), where a clear slow rise is observed consistent with a slow accumulation of the S_1 population. The first excited singlet fluorescence rise and decay were described with multiexponential terms with $\tau_1 = 2.8$ ps (rise), $\tau_2 = 7.5$ ps (decay), and $\tau_3 = 57$ ps (decay, lifetime). We notice that the 2.8 ps growth is not identical to the 5.4 ps decay observed for the S_2 emission. This could be due to the fact that the S_1 state also undergoes rapid vibrational relaxation, or it may correspond to a kind of average between the 1 and 5.4 ps components observed for the S_2 emission. In any case, some spectral evolution is expected as the S_1 state is populated by internal conversion. Such spectral evolution can also be related to the relaxation of the solvent shells around the electron density distribution of the fluorescent state (ethanol, with solvent relaxation components in the range from subpicoseconds to more than 10 ps). All these relaxation events are likely to produce modulations in the intensity of the S_1 emission at the detection wavelength. It is clear however that the accumulation of the S_1 population is not instantaneous given its formation due to internal conversion from a somewhat long-lived S_2 state.

The 4QC5 molecule shows the same general of behavior as 4QC3; however, the overall time for the S_2 – S_1 conversion is slightly faster, having time constants of $\tau_1 = 0.5$ ps and $\tau_2 = 2.9$ ps for the second excited singlet decay. For 4QC5 the S_1 signal accumulation is again consistent with a slow population growth as shown in the inset of Figure 7C. The excitation with 266 nm light is again included in the inset with similar observations as in the 4QC3 molecule. In summary, for the 4QC series, the slowest S_2 – S_1 conversion was observed for the medium size cyanine 4QC3 with a somewhat faster process for 4QC5 and ultrafast decay for the shortest cyanine 4QC1.

The up-conversion results for the TC family are shown in Figure 8. Again, in congruence with the observations for the

4QC series, the fastest dynamics are seen for the shortest cyanine TC3 which has a fast 1.5 ps single-exponential S_2 decay and a 2.2 ps growth of the S_1 state as shown in the inset of Figure 8A. The TC cyanine of intermediate size: TC5 actually shows by far the slowest S_2 decay of all the cyanines, with time constants of $\tau_1 = 1.9$ ps and $\tau_2 = 17.3$ ps. The corresponding slow S_1 accumulation was also verified and is included in the inset of Figure 8B. The 17.3 ps we observed for the second component is consistent with a previous report on the lifetime of the S_2 state of this cyanine, determined through transient absorption with picoseconds resolution.¹⁶ Similarly to the 4QC series, the longest cyanine (here TC7) shows S_2 decays in an intermediate time scale in comparison with TC3 (fastest) and TC5 (slowest). This is summarized in Table 1.

The overall tendencies of the S_2 states in the three cyanine series can be easily understood according to the following considerations: the structures of two shortest quinolyl cyanines 2QC1 and 4QC1 have been studied by X-ray crystallography. These compounds have been shown to be highly distorted from planarity due to steric hindrance between the aromatic end groups.^{44,47–50} It has been established previously that such distortion from planarity makes these systems have fast and efficient photoisomerization channels upon electronic excitation.^{37–39,42,43,51–54} More specifically, it has been shown that the nonplanar geometries of 2QC1 and 4QC1 allow a fast and predirected evolution in the potential energy surfaces toward conical intersections which drives the loss of population of the S_1 states. It is easy to translate this behavior to the S_2 dynamics observed herein for 2QC1 and 4QC1: their nonplanar geometries are associated with rapid evolution in the S_2 surface, moving to geometries with a large S_2 – S_1 coupling and thereby defining short S_2 lifetimes.

The rest of the cyanines of this study are planar according to previous studies.^{24,35,44,47,49,55–57} The planar cyanines, 2QC3–5, 4QC3–5, and the TC series actually show a clear systematic trend in relation to their S_2 lifetimes as elaborated next: the energy gap between the first and second singlet excited states

can be estimated for most of these compounds using the steady state emission observed from the S_2 state. The S_2 – S_1 gap was thus determined as the difference between the energy of the S_2 emission and that of the regular S_1 fluorescence (notice that the absorption spectra are significantly crowded with vibroelectronic peaks in this region, making it uncertain to establish the S_2 energy from these spectra). The ordering of the planar cyanines of our study with respect to their energy gap (S_2 – S_1) is the following in order of decreasing gap: TC5, 4QC3, TC7, Cl-TC7, 4QC5, TC3, 2QC3, and 2QC5 (see below).

The log of the S_2 decay rates are plotted as a function of the S_2 – S_1 energy gaps for these cyanines in Figure 9. As can be

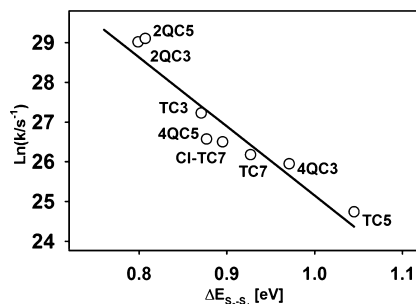


Figure 9. Experimental S_2 – S_1 internal conversion rate constants (logarithmic scale) as a function of the S_2 – S_1 energy gap for the cyanines of this study. The continuous line shows the linear trend for the data with a correlation coefficient of $r = 0.95$.

seen, a nice linear trend is observed with a correlation coefficient of $r = 0.95$, consistent with the second excited singlet having lifetimes governed by the energy gap law with respect to the S_1 state.^{58,59}

$$k_{IC} = C \exp\left(-\gamma \frac{\Delta E_{2-1}}{h\omega_m}\right)$$

where C is a pre-exponential factor that measures the electronic coupling matrix element, ΔE_{2-1} is the energy difference between the S_2 and the S_1 states, $h\omega_m$ is the energy of the vibrational mode in the acceptor state, and γ is related to the degree of displacement of the potential energy surfaces between the two states. From the large similarity of the cyanine's bridges and previously studied polyenic molecules, the relevant acceptor mode can be postulated to be the $C=C$ stretching mode.⁵⁹ It should be noticed that the trend shown in Figure 9 involves different types of cyanines with different conjugation sizes and different end groups. To our knowledge, this is the first time the energy gap law is recognized for the S_2 – S_1 internal conversion in cyanines. Such observation should serve as the primary variable in the design of cyanines with long S_2 lifetimes, which, as mentioned previously, are of interest in energy or electron transfer applications.^{13,17,19,60,61}

We have additionally tested how an increase of the viscosity of the solvent media may affect the S_2 lifetimes. In order to keep a similar hydrogen bonding environment to the ethanol solvent (viscosity: 1.2 mPa·s), we made up-conversion measurements in ethylene glycol at room temperature (viscosity: 16 mPa·s). The results are summarized in Figure 10 and Table 2. As can be seen, in the more viscous ethylene glycol solutions, the S_2 decays show clear but not major differences in comparison with the ethanol solutions. In particular, for the 4QC3 cyanine, the time constants go from

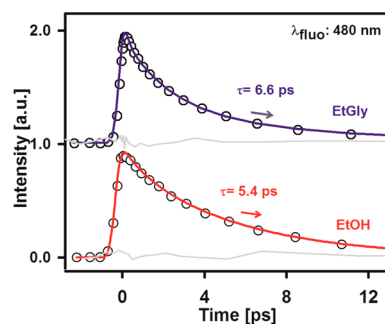


Figure 10. Time-resolved fluorescence results for 4QC3 in different solvents (ethylene glycol (EtGly) and ethanol (EtOH)). The detection wavelength (λ_{fluor}) is indicated. The gray lines are the solvent-only signal detected at this λ_{fluor} .

Table 2. Parameters for the Decay of the S_2 State for Diverse Cyanines in Ethylene Glycol Solutions

cyanine	λ_{fluor} [nm]	τ_1 [ps]	a_1	τ_2 [ps]	a_2
TC5 ^a	435	2.1 ± 0.1	0.52	17.5 ± 0.9	0.48
TC7 ^b	500	<0.3	0.52	5.0 ± 0.3	0.48
4QC3 ^b	480	1.6 ± 0.07	0.84	6.6 ± 0.3	0.16
2QC3 ^b	500	<0.2	1		

^a $\lambda_{\text{exc}} = 266$ nm. ^b $\lambda_{\text{exc}} = 400$ nm.

1.0 and 5.4 ps in ethanol to 1.6 and 6.6 ps in ethylene glycol, while for TC5, they go from 1.9 and 17.3 ps in ethanol to 2.1 and 17.5 ps in ethylene glycol. Results for TC7 and 2QC3 in ethylene glycol are also included in Table 2.

The overall change in the S_2 decays (considering the longer component in the decay) is between 1% and 22%, showing some effect of the viscosity in the S_2 lifetimes. This effect is thus related to a reduction of the rate of geometry changes in the S_2 surface after excitation.^{14,26} While the solvent viscosity certainly has an effect on the S_2 lifetimes, from the clear verification of the energy gap law in Figure 9, it is clear that the S_2 – S_1 energy gaps are much clearer predictors of the S_2 lifetimes.

Since the objective of our study was to determine which kind of cyanines may have long S_2 lifetimes, for electron and energy transfer from S_2 applications, we have measured the S_2 decays of the heptamethine cyanine chlorinated at the meso position shown in Figure 11 (Cl-TC7). This compound is interesting from two points of view. First, it contains a labile chloride in the meso position, from which the cyanine can be easily functionalized to include electron and/or energy acceptors in future molecular designs for one- and two-photon sensitization.^{13,17,60} In the second place, Cl-TC7 contains a rigidized middle section thanks to the six-membered cycle that joins carbons 3' and 5', limiting their relative mobility. The steady state and fluorescence up-conversion results for this compound are included in Figure 11. The time constants for the biexponential decay were determined to be <0.4 and 3.1 ps. These times are comparable and even slightly faster than those of the analogous compound TC7 which does not possess the middle cyclic system. Given the similarities between the dynamics of these two compounds, it can be concluded that the S_2 decays are not strongly influenced by the geometry restrictions imparted at the central region in the Cl-TC7 cyanine. On the other hand, the S_2 lifetime in this compound follows the aforementioned energy gap law in Figure 9 and remains in the picoseconds regime; a time scale large enough for energy or electron transfer events to donor molecules which

Table 3. Parameters for the Decay of the S_2 and S_1 States of Cl-TC7 in Ethanol Solutions

state detected	λ_{fluo} [nm]	τ_1 [ps]	a_1	τ_2 [ps]	a_2	τ_3 [ps]	a_3
S_2^b	500	<0.4	0.74	3.1 ± 0.2	0.26		
S_2^a	530	<0.3	0.58	3.1 ± 0.4	0.42		
S_1^b	870	2.7 ± 0.02	-0.50	6.0 ± 0.2	0.28	720 ± 20	0.22

^a $\lambda_{\text{exc}} = 266$ nm. ^b $\lambda_{\text{exc}} = 400$ nm.

Table 4. Parameters for the Fluorescence Decay of the S_2 State upon Two-Photon Excitation at 800 nm for Three Cyanines in Ethanol Solutions

cyanine	λ_{fluo} [nm]	τ_1 [ps]	a_1	τ_2 [ps]	a_2
2QC3	460	<0.3	1		
4QC3	480	1.0 ± 0.07	0.85	5.1 ± 0.9	0.15
TC5	435	0.6 ± 0.06	0.71	15.6 ± 2	0.29

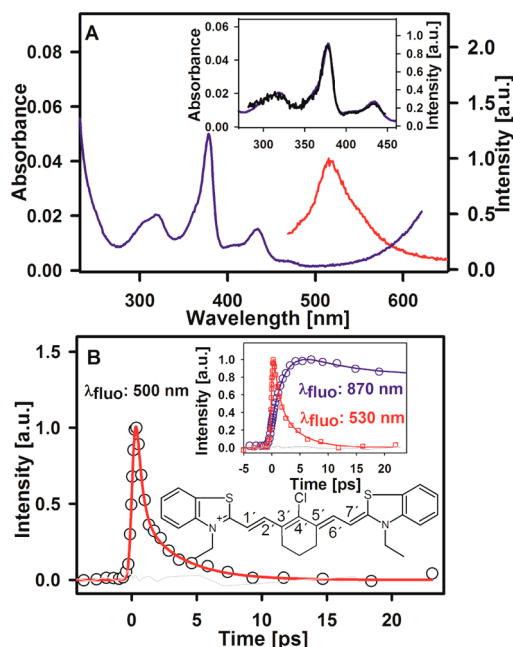


Figure 11. (A) Absorption (blue), corrected emission (red, $\lambda_{\text{exc}} = 375$ nm), and excitation (black, inset, $\lambda_{\text{det}} = 530$ nm) spectra of the S_2 state of Cl-TC7 (structure shown). (B) Detection of the S_2 state emission with femtosecond fluorescence up-conversion (red, $\lambda_{\text{exc}} = 400$ nm). Inset: time-resolved fluorescence from the S_1 (blue) and from the S_2 (red) states ($\lambda_{\text{exc}} = 266$ nm). The detection wavelengths (λ_{fluo}) are indicated. The gray lines are the solvent-only scans.

can be bonded at a very near distance as substituents at the meso position.

Finally, we have performed several experiments where the cyanines were excited by degenerate two-photon absorption with 800 nm pulses. The results for 2QC3, 4QC3, and TC5 are included in Figure 12. The excitation of these molecules with two photons is an efficient process since, as has been established previously,^{23,25,26,62–67} the excited states in the respective energy region have large cross sections for this nonlinear excitation. Such is granted by the symmetry relations of the states, taking the first singlet as an intermediate out of resonance transition with a sharp onset, ideal for the 800 nm two-photon excitation (see refs 22–28 and 62–67 for detailed descriptions of the nonlinear optical properties of cyanines and related compounds). For cyanines 4QC3 and TC5, we have measured the two-photon absorption cross sections according

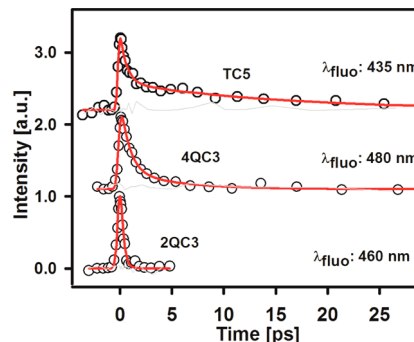


Figure 12. Time-resolved fluorescence S_2 emission from two-photon excitation at 800 nm for 2QC3, 4QC3, and TC5. The detection wavelengths (λ_{fluo}) are indicated. The gray lines are the solvent-only scans.

to the method in the Supporting Information. The resulting values for 800 nm excitation are 321 GM for TC5 and 187 GM for 4QC3, confirming that these compounds have significant two-photon cross sections at the excitation wavelength.

The up-conversion experiments in Figure 12 are among the first ones to time-resolve emission with femtosecond resolution after two-photon excitation and the first ones to detect upper state emissions after two-photon excitation.²⁶ Because of the difficulty of these experiments and the position of the S_1 absorptions, here we only studied the two cyanines with the slowest S_2 decays plus 2QC3 as a representative member of the 2Q series. As can be seen, the S_2 dynamics from compounds 2QC3, 4QC3, and TC5 in these experiments are similar to those obtained with direct single-photon excitation with 400 or 266 nm light. The time constants for the 4QC3 system are 1.0 and 5.1 ps. For 2QC3 the S_2 lifetime remained below 0.3 ps, and for TC5 the time constants are 0.6 and 15.6 ps. The experiments of Figure 12 demonstrate the feasibility of forming a relatively long-lived (picoseconds) upper excited state with the absorption of two photons at 800 nm, potentially allowing for electron or energy transfer events from S_2 after the nonlinear excitation.

CONCLUSIONS

We present the first detailed characterization of the dynamics of the upper excited states in cyanines with femtosecond resolution. It was observed that the shortest cyanines 2QC1 and 4QC1 have ultrafast (<0.4 ps) S_2 lifetimes, with a correspondingly fast population of their S_1 states. For these short cyanines, the rapid dynamics are associated with the fact that their ground state geometry is nonplanar due to steric hindrance between the end groups.^{47,48,50} This distortion predisposes the systems to rapid decays in the upper states given that the resulting wave packet evolves directly to regions of high S_2 – S_1 coupling.⁴⁴

On the other hand, the rest of the cyanines of our study are planar and, for the three series 2QC, 4QC, and TC, the energy gap rule is strictly followed. From the S_2 – S_1 gaps, it results that

for the 4QC and TC cyanines the medium size molecules (4QC3 and TC5) have the longest S_2 lifetimes within their series. Particularly, TC5, the cyanine with the largest gap, is the one with the overall slowest S_2 decay of all the compounds of this study, with a lifetime component of 17.3 ps in ethanol.

The influence of the solvent viscosity was tested through comparisons between ethanol and ethylene glycol solutions. Although differences among these two solvents are observed, the upper state lifetimes do not show dramatic changes upon the increment of viscosity from 1.2 mPa·s in ethanol to 16 mPa·s in ethylene glycol. Though certainly there is an influence of viscosity, the above-mentioned trend which follows the energy gap rule implies that it is the relative energies of S_2 and S_1 energies what most closely determines the upper state dynamics. Additionally, we verified that the S_2 states can have lifetimes in the picoseconds region, independently of whether near direct S_2 excitation is made (400 nm), an upper singlet state is formed (S_n with $n > 2$ formation with 266 nm light), or degenerate two-photon excitation is made with 800 nm femtosecond pulses.

The present characterization isolates for the first time several of the variables that determine the lifetime of the upper singlets in symmetric cyanines. Transfer of energy and/or electrons from such upper states has been considered of potential relevance in photosensitization and photovoltaic applications. Our experiments set the design variables for such systems, pointing to the energy gap law as the most relevant factor determining the upper state dynamics for the planar cyanines, while for the nonplanar ones, the S_2 states undergo ultrafast internal conversion to the first singlet excited state.

S_2 lifetimes of many picoseconds may allow for efficient processes from these states before relaxation to the first excited state takes place, thereby opening the possibility of using the near 1 eV electronic energy difference between these two states.

■ ASSOCIATED CONTENT

● Supporting Information

S_2 emission spectra for 2QC1, 2QC3, 2QC5, 4QC1, and TC3 in ethanol solutions, experimental data for the energy gap and S_2 – S_1 internal conversion rate, experimental procedures for the determination of the two-photon absorption coefficients of TC5 and 4QC3, up-conversion results at additional wavelengths, and full refs 23, 28, and 67. This material is available free of charge via the Internet at <http://pubs.acs.org>.

■ AUTHOR INFORMATION

Corresponding Author

*E-mail jpeon@servidor.unam.mx (J.P.).

Notes

The authors declare no competing financial interest.

■ ACKNOWLEDGMENTS

For financial support we thank CONACyT Grant 178541 and PAPIIT-UNAM Grant IN 204211.

■ REFERENCES

- (1) Özhalıcı-Ünal, H.; Pow, C. L.; Marks, S. A.; Jesper, L. D.; Silva, G. L.; Shank, N. I.; Jones, E. W.; Burnette, J. M.; Berget, P. B.; Armitage, B. A. A Rainbow of Fluoromolecules: A Promiscuous scFv Protein Binds to and Activates a Diverse Set of Fluorogenic Cyanine Dyes. *J. Am. Chem. Soc.* **2008**, *130*, 12620–12621.
- (2) Luby-Phelps, K.; Mujumdar, S.; Mujumdar, R. B.; Ernst, L. A.; Galbraith, W.; Waggoner, A. S. A Novel Fluorescence Ratiometric Method Confirms the Low Solvent Viscosity of the Cytoplasm. *Biophys. J.* **1993**, *65*, 236–242.
- (3) Wainwright, M.; Kristiansen, J. E. Quinoline and Cyanine Dyes: Putative Anti-MRSA Drugs. *Int. J. Antimicrob. Agents* **2003**, *22*, 479–486.
- (4) Luo, S.; Zhang, E.; Su, Y.; Cheng, T.; Shi, C. A Review of NIR Dyes in Cancer Targeting and Imaging. *Biomaterials* **2011**, *32*, 7127–7138.
- (5) Zhan, W.-h.; Wu, W.-j.; Hua, J.-l.; Jing, Y.-h.; Meng, F.-s.; Tian, H. Photovoltaic Properties of New Cyanine-Naphthalimide Dyads Synthesized by ‘Click’ Chemistry. *Tetrahedron Lett.* **2007**, *48*, 2461–2465.
- (6) Castro, F. A.; Faes, A.; Geiger, T.; Graeff, C. F. O.; Nagel, M.; Nüesch, F.; Hany, R. On the Use of cyanine Dyes as Low-bandgap Materials in Bulk Heterojunction Photovoltaic Devices. *Synth. Met.* **2006**, *156*, 973–978.
- (7) Sun, R.; Yan, B.-L.; Ge, J.-F.; Xu, Q.-f.; Li, N.-J.; Wu, X.-Z.; Song, Y.-L.; Lu, J.-M. Third-Order Nonlinear Optical Properties of Unsymmetric Pentamethine Cyanine Dyes Possessing Benzoxazolyl and Benzothiazolyl Groups. *Dyes Pigm.* **2013**, *96*, 189–195.
- (8) Zheng, Q.; He, G. S.; Prasad, P. N. A Novel Near IR Two-Photon Absorbing Chromophore: Optical Limiting and Stabilization Performances at an Optical Communication Wavelength. *Chem. Phys. Lett.* **2009**, *475*, 250–255.
- (9) Bazylińska, U.; Pietkiewicz, J.; Saczko, J.; Nattich-Rak, M.; Rossowska, J.; Garbiec, A.; Wilk, K. A. Nanoemulsion-Templated Multilayer Nanocapsules for Cyanine-Type Photosensitizer Delivery to Human Breast Carcinoma Cells. *Eur. J. Pharm. Sci.* **2012**, *47*, 406–420.
- (10) Bouit, P.-A.; Aronica, C.; Toupet, L. C.; Le Guennic, B.; Andraud, C.; Maury, O. Continuous Symmetry Breaking Induced by Ion Pairing Effect in Heptamethine Cyanine Dyes: Beyond the Cyanine Limit. *J. Am. Chem. Soc.* **2010**, *132*, 4328–4335.
- (11) Fabian, J.; Hartmann, H. *Light Absorption of Organic Colorants: Theoretical Treatment and Empirical Rules*, AAA ed.; Springer-Verlag: New York, 1980.
- (12) Kasha, M. Characterization of Electronic Transitions in Complex Molecules. *Discuss. Faraday Soc.* **1950**, *9*, 14–19.
- (13) Bouit, P.-A.; Spaenig, F.; Kuzmanich, G.; Krokos, E.; Oelsner, C.; García-Garibay, M. A.; Delgado, J. L.; Martin, N.; Guldí, D. M. Efficient Utilization of Higher-Lying Excited States to Trigger Charge-Transfer Events. *Chem.—Eur. J.* **2010**, *16*, 9638–9645.
- (14) Kasatani, K.; Sato, H. Viscosity-Dependent Decay Dynamics of the S_2 State of Cyanine Dyes with 3, 5, and 7 Methine Units by Picosecond Fluorescence Lifetime Measurements. *Bull. Chem. Soc. Jpn.* **1996**, *69*, 3455–3460.
- (15) Řehák, V.; Novák, A.; Titz, M. $S_2 \rightarrow S_0$ Fluorescence of Cryptocyanine Solutions. *Chem. Phys. Lett.* **1977**, *52*, 39–42.
- (16) Oulianov, D. A.; Dvornikov, A. S.; Rentzepis, P. M. Optical Limiting and Picosecond Relaxation of Carbocyanines Upper Electronic States. *Opt. Commun.* **2002**, *205*, 427–436.
- (17) Kesti, T.; Tkachenko, N.; Yamada, H.; Imahori, H.; Fukuzumi, S.; Lemmetyinen, H. C70vs. C60 in Zinc Porphyrin-Fullerene Dyads: Prolonged Charge Separation and Ultrafast Energy Transfer from the Second Excited Singlet State of Porphyrin. *Photochem. Photobiol. Sci.* **2003**, *2*, 251–258.
- (18) Mataga, N.; Chosrowjan, H.; Shibata, Y.; Yoshida, N.; Osuka, A.; Kikuzawa, T.; Okada, T. First Unequivocal Observation of the Whole Bell-Shaped Energy Gap Law in Intramolecular Charge Separation from S_2 Excited State of Directly Linked Porphyrin–Imide Dyads and Its Solvent-Polarity Dependencies. *J. Am. Chem. Soc.* **2001**, *123*, 12422–12423.
- (19) LeGourriérec, D.; Andersson, M.; Davidsson, J.; Mukhtar, E.; Sun, L.; Hammarström, L. Photoinduced Electron Transfer from a Higher Excited State of a Porphyrin in a Zinc Porphyrin–Ruthenium(II) Tris-bipyridine Dyad. *J. Phys. Chem. A* **1999**, *103*, 557–559.
- (20) Petersson, J.; Eklund, M.; Davidsson, J.; Hammarström, L. Variation of Excitation Energy Influences the Product Distribution of a Two-Step Electron Transfer: S_2 vs S_1 Electron Transfer in a

Zn(II)porphyrin–Viologen Complex. *J. Am. Chem. Soc.* **2009**, *131*, 7940–7941.

(21) Gaikwad, P. On the Optical Limiting and Z-Scan of Hexamethylindotricarbocyanine Perchlorate Dye. *Opt. Mater.* **2009**, *31*, 1559–1563.

(22) Bouit, P.-A.; Wetzels, G.; Berginc, G.; Loiseaux, B.; Toupet, L.; Feneyrou, P.; Bretonnière, Y.; Kamada, K.; Maury, O.; Andraud, C. Near IR Nonlinear Absorbing Chromophores with Optical Limiting Properties at Telecommunication Wavelengths. *Chem. Mater.* **2007**, *19*, 5325–5335.

(23) Padilha, L. A.; Webster, S.; Przhonska, O. V.; Hu, H.; Peceli, D.; Rosch, J. L.; Bondar, M. V.; Gerasov, A. O.; Kovtun, Y. P.; Shandura, M. P.; et al. Nonlinear Absorption in a Series of Donor-p-Acceptor Cyanines with Different Conjugation Lengths. *J. Mater. Chem.* **2009**, *19*, 7503–7513.

(24) Fu, J.; Padilha, L. A.; Hagan, D. J.; Van Stryland, E. W.; Przhonska, O. V.; Bondar, M. V.; Slominsky, Y. L.; Kachkovski, A. D. Experimental and Theoretical Approaches to Understanding Two-Photon Absorption Spectra in Polymethine and Squaraine Molecules. *J. Opt. Soc. Am. B* **2007**, *24*, 67–76.

(25) Przhonska, O.; Webster, S.; Padilha, L.; Hu, H.; Kachkovski, A.; Hagan, D.; Stryland, E. Two-Photon Absorption in Near-IR Conjugated Molecules: Design Strategy and Structure–Property Relations. In *Advanced Fluorescence Reporters in Chemistry and Biology I*; Demchenko, A. P., Ed.; Springer: Berlin, 2010; pp 105–147.

(26) Kasatani, K.; Kawasaki, M.; Sato, H. Short-Wavelength Fluorescence Caused by Sequential Two-Photon Excitation of Some Cyanine Dyes: Effect of Solvent Viscosity on the Quantum Yields. *Chem. Phys.* **1984**, *83*, 461–469.

(27) Przhonska, O. V.; Lim, J. H.; Hagan, D. J.; Van, S. E. W.; Bondar, M. V.; Slominsky, Y. L. Nonlinear Light Absorption of Polymethine Dyes in Liquid and Solid Media. *J. Opt. Soc. Am. B* **1998**, *15*, 802–809.

(28) Hu, H.; Fishman, D. A.; Gerasov, A. O.; Przhonska, O. V.; Webster, S.; Padilha, L. A.; Peceli, D.; Shandura, M.; Kovtun, Y. P.; Kachkovski, A. D.; et al. Two-Photon Absorption Spectrum of a Single Crystal Cyanine-Like Dye. *J. Phys. Chem. Lett.* **2012**, *3*, 1222–1228.

(29) Pais, I. R.; Nunes, M. J.; Reis, L. V.; Santos, P. F.; Almeida, P. The synthesis of Chloroheptamethinecyanine Dyes in the Absence of Water. *Dyes Pigm.* **2008**, *77*, 48–52.

(30) Li, M.; Pacey, G. E. Spectrophotometric Determination of Trace Water in Organic Solvents with a Near Infrared Absorbing Dye. *Talanta* **1997**, *44*, 1949–1958.

(31) Zugazagoitia, J. S.; Collado-Fregoso, E.; Plaza-Medina, E. F.; Peon, J. Relaxation in the Triplet Manifold of 1-Nitronaphthalene Observed by Transient Absorption Spectroscopy. *J. Phys. Chem. A* **2009**, *113*, 805–810.

(32) Plaza-Medina, E. F.; Rodríguez-Córdoba, W.; Morales-Cueto, R.; Peon, J. Primary Photochemistry of Nitrated Aromatic Compounds: Excited-State Dynamics and NO \cdot Dissociation from 9-Nitroanthracene. *J. Phys. Chem. A* **2011**, *115*, 577–585.

(33) Rodríguez-Córdoba, W.; Noria, R.; Guarín, C. A.; Peon, J. Ultrafast Photosensitization of Phthalocyanines through Their Axial Ligands. *J. Am. Chem. Soc.* **2011**, *133*, 4698–4701.

(34) Zugazagoitia, J. S.; Almora-Díaz, C. X.; Peon, J. Ultrafast Intersystem Crossing in 1-Nitronaphthalene. An Experimental and Computational Study. *J. Phys. Chem. A* **2008**, *112*, 358–365.

(35) Park, J. AM1 Semiempirical Calculated Potential Energy Surfaces for the Isomerization of Symmetrical Carbocyanines. *Dyes Pigm.* **2000**, *46*, 155–161.

(36) Yartsev, A.; Alvarez, J.-L.; Åberg, U.; Sundström, V. Overdamped Wavepacket Motion Along a Barrierless Potential Energy Surface in Excited State Isomerization. *Chem. Phys. Lett.* **1995**, *243*, 281–289.

(37) Zhang, T.; Chen, C.; Gong, Q.; Yan, W.; Wang, S.; Yang, H.; Jian, H.; Xu, G. Time-Resolved Excited State Dynamics of a Cyanine Dye. *Chem. Phys. Lett.* **1998**, *298*, 236–240.

(38) Petrov, N. K.; Gulakov, M. N.; Alfimov, M. V.; Busse, G.; Frederichs, B.; Techert, S. Photophysical Properties of 3,3'-

Diethylthiacarbocyanine Iodide in Binary Mixtures. *J. Phys. Chem. A* **2003**, *107*, 6341–6344.

(39) Sahyun, M. R. V.; Serpone, N. Photophysics of Thiocarbocyanine Dyes: Relaxation Dynamics in a Homologous Series of Thiocarbocyanines. *J. Phys. Chem. A* **1997**, *101*, 9877–9883.

(40) Dietzek, B.; Yartsev, A.; Tarnovsky, A. N. Watching Ultrafast Barrierless Excited-State Isomerization of Pseudocyanine in Real Time. *J. Phys. Chem. B* **2007**, *111*, 4520–4526.

(41) Maruszewski, K.; Jasierski, M.; Stręk, W. Spectroscopic Behavior of 1,1'-Diethyl-2,2'-Diodide in Ethanol/Water Solutions with High Ionic Strength. *J. Mol. Struct.* **2002**, *610*, 187–190.

(42) Sanchez-Galvez, A.; Hunt, P.; Robb, M. A.; Olivucci, M.; Vreven, T.; Schlegel, H. B. Ultrafast Radiationless Deactivation of Organic Dyes: Evidence for a Two-State Two-Mode Pathway in Polymethine Cyanines. *J. Am. Chem. Soc.* **2000**, *122*, 2911–2924.

(43) Dietzek, B.; Christensson, N.; Pascher, T.; Pullerits, T.; Yartsev, A. Ultrafast Excited-State Isomerization Dynamics of 1,1'-Diethyl-2,2'-Cyanine Studied by Four-Wave Mixing Spectroscopy. *J. Phys. Chem. B* **2007**, *111*, 5396–5404.

(44) Tredwell, C. J.; Keary, C. M. Picosecond Time Resolved Fluorescence Lifetimes of the Polymethine and Related Dyes. *Chem. Phys.* **1979**, *43*, 307–316.

(45) Marks, A. F.; Noah, A. K.; Sahyun, M. R. V. Bond-Length Alternation in Symmetrical Cyanine Dyes. *J. Photochem. Photobiol. A* **2001**, *139*, 143–149.

(46) Sundström, V.; Gillbro, T. Viscosity Dependent Radiationless Relaxation Rate of Cyanine Dyes. A Picosecond Laser Spectroscopy Study. *Chem. Phys.* **1981**, *61*, 257–269.

(47) Brooker, L. G. S.; White, F. L.; Sprague, R. H.; Dent, S. G., Jr.; Van, Z. G. Steric Hindrance to Planarity in Dye Molecules. *Chem. Rev.* **1947**, *41*, 325–351.

(48) Yoshioka, H.; Nakatsu, K. Crystal Structures of Two Photographic Sensitizing Dyes, 1,1'-Diethyl-2,2'-Cyanine Bromide and 1,1'-Diethyl-4,4'-Cyanine Bromide. *Chem. Phys. Lett.* **1971**, *11*, 255–258.

(49) Iwasaki, M.; Kita, M.; Ito, K.; Kohno, A.; Fukunishi, K. Intercalation Characteristics of 1,1'-Diethyl-2,2'-Cyanine and other Cationic Dyes in Synthetic Saponite: Orientation in the Interlayer. *Clays Clay Miner.* **2000**, *48*, 392–399.

(50) Marchetti, A. P.; Salzberg, C. D.; Walker, E. I. P. The Optical Properties of Crystalline 1,1'-Diethyl-2,2'-Cyanine Iodide. *J. Chem. Phys.* **1976**, *64*, 4693–4698.

(51) Chapman, G.; Henary, M.; Patonay, G. The Effect of Varying Short-Chain Alkyl Substitution on the Molar Absorptivity and Quantum Yield of Cyanine Dyes. *Anal. Chem. Insights* **2011**, *6*, 29–36.

(52) Serpone, N.; Sahyun, M. R. V. Photophysics of Dithiacarbocyanine Dyes: Subnanosecond Relaxation Dynamics of a Dithia-2,2'-Carbocyanine Dye and its 9-Methyl-Substituted Meso Analog. *J. Phys. Chem.* **1994**, *98*, 734–737.

(53) Weigel, A.; Pfaffe, M.; Sajadi, M.; Mahrwald, R.; Improt, R.; Barone, V.; Polli, D.; Cerullo, G.; Ernström, N. P.; Santoro, F. Barrierless Photoisomerisation of the “Simplest Cyanine”: Joining Computational and Femtosecond Optical Spectroscopies to Trace the Full Reaction Path. *Phys. Chem. Chem. Phys.* **2012**, *14*, 13350–13364.

(54) Vladimirova, K. G.; Freidzon, A. Y.; Bagatur-yants, A. A.; Zakharova, G. V.; Chibisov, A. K.; Alfimov, M. V. Modeling the Structure, Absorption Spectra, and Cis-Trans Isomerization of Thiocarbocyanine Dyes. *High Energy Chem.* **2008**, *42*, 275–282.

(55) Meyer, Y. H.; Pittman, M.; Plaza, P. Transient Absorption of Symmetrical Carbocyanines. *J. Photochem. Photobiol. A* **1998**, *114*, 1–21.

(56) Shi, Q.-Q.; Sun, R.; Ge, J.-F.; Xu, Q.-F.; Li, N.-J.; Lu, J.-M. A Comparative Study of Symmetrical and Unsymmetrical Trimethine Cyanine Dyes Bearing Benzoxazolyl and Benzothiazolyl Groups. *Dyes Pigm.* **2012**, *93*, 1506–1511.

(57) Emerson, E. S.; Conlin, M. A.; Rosenoff, A. E.; Norland, K. S.; Rodriguez, H.; Chin, D.; Bird, G. R. The Geometrical Structure and Absorption Spectrum of a Cyanine Dye Aggregate. *J. Phys. Chem.* **1967**, *71*, 2396–2403.

- (58) Mimuro, M.; Akimoto, S.; Takaichi, S.; Yamazaki, I. Effect of Molecular Structures and Solvents on the Excited State Dynamics of the S_2 State of Carotenoids Analyzed by the Femtosecond Up-Conversion Method. *J. Am. Chem. Soc.* **1997**, *119*, 1452–1453.
- (59) Akimoto, S.; Yamazaki, I.; Takaichi, S.; Mimuro, M. Excitation Relaxation Dynamics of Linear Carotenoids. *J. Lumin.* **2000**, *87–89*, 797–799.
- (60) Macpherson, A. N.; Arellano, J. B.; Fraser, N. J.; Cogdell, R. J.; Gillbro, T. Efficient Energy Transfer from the Carotenoid S_2 State in a Photosynthetic Light-Harvesting Complex. *Biophys. J.* **2001**, *80*, 923–930.
- (61) Mataga, N.; Taniguchi, S.; Chosrowjan, H.; Osuka, A.; Yoshida, N. Ultrafast Charge Transfer and Radiationless Relaxations from Higher Excited State (S_2) of Directly Linked Zn-Porphyrin (ZP)-Acceptor Dyads: Investigations into Fundamental Problems of Exciplex Chemistry. *Chem. Phys.* **2003**, *295*, 215–228.
- (62) Sissa, C.; Jahani, P. M.; Soos, Z. G.; Painelli, A. Essential State Model for Two-Photon Absorption Spectra of Polymethine Dyes. *ChemPhysChem*. **2012**, *13*, 2795–2800, S2795/2791–S2795/2795.
- (63) Fuyuki, M.; Furuta, K.; Wada, A. Control of Reaction Efficiency by Two-Color Two-Pulse Excitation: Photoisomerization of Indocyanine Green in Condensed Phase. *Chem. Phys. Lett.* **2011**, *511*, 45–50.
- (64) Kim, C. H.; Joo, T. Ultrafast Time-Resolved Fluorescence by Two Photon Absorption Excitation. *Opt. Express* **2008**, *16*, 20742–20747.
- (65) Webster, S.; Fu, J.; Padilha, L. A.; Przhonska, O. V.; Hagan, D. J.; Van Stryland, E. W.; Bondar, M. V.; Slominsky, Y. L.; Kachkovski, A. D. Comparison of Nonlinear Absorption in Three Similar Dyes: Polymethine, Squaraine and Tetraone. *Chem. Phys.* **2008**, *348*, 143–151.
- (66) Lepkowicz, R. S.; Przhonska, O. V.; Hales, J. M.; Fu, J.; Hagan, D. J.; Van Stryland, E. W.; Bondar, M. V.; Slominsky, Y. L.; Kachkovski, A. D. Nature of the Electronic Transitions in Thiocarbocyanines with a Long Polymethine Chain. *Chem. Phys.* **2004**, *305*, 259–270.
- (67) Webster, S.; Peceli, D.; Hu, H.; Padilha, L. A.; Przhonska, O. V.; Masunov, A. E.; Gerasov, A. O.; Kachkovski, A. D.; Slominsky, Y. L.; Tolmachev, A. I.; et al. Near-Unity Quantum Yields for Intersystem Crossing and Singlet Oxygen Generation in Polymethine-Like Molecules: Design and Experimental Realization. *J. Phys. Chem. Lett.* **2010**, *1*, 2354–2360.